

Fast Solution of Volume–Surface Integral Equation for Scattering from Composite Conducting–Dielectric Targets Using Multilevel Fast Dipole Method

Xinlei Chen, Changqing Gu, Zhenyi Niu, Zhuo Li

College of Electronic and Information Engineering, Nanjing University of Aeronautics and Astronautics, Nanjing 210016, People's Republic of China

Received 18 July 2011; accepted 14 December 2011

ABSTRACT: This article presents a fast solution to the volume–surface integral equation for electromagnetic scattering from three-dimensional (3D) targets comprising both conductors and dielectric materials by using the multilevel fast dipole method (MLFDM). This scheme is based on the concept of equivalent dipole-moment method (EDM) that views the Rao–Wilton–Glisson and the Schaubert–Wilton–Glisson basis functions as dipole models with equivalent dipole moments. In the MLFDM, a simple Taylor's series expansion of the terms R^α ($\alpha = 1, -1, -2, -3$) and $\hat{R}\hat{R}$ in the formulation of the EDM transforms the interaction between two equivalent dipoles into an aggregation–translation–disaggregation form naturally. Furthermore, benefiting from the multilevel grouping scheme, the matrix-vector product can be accelerated and the memory cost is reduced remarkably. Simulation results are presented to demonstrate the efficiency and accuracy of this method. © 2012 Wiley Periodicals, Inc. *Int J RF and Microwave CAE* 22:624–631, 2012.

Keywords: electromagnetic scattering (EM); volume–surface integral equation (VSIE); method of moments (MoM); equivalent dipole-moment method (EDM); multilevel fast dipole method (MLFDM)

I. INTRODUCTION

The scattering of electromagnetic waves from composite conducting–dielectric targets has been an important research area because of its wide applications such as radiation of various antennas with dielectric radomes, scattering of invisible aircrafts coated with absorbing materials, and microstrip structures on finite anisotropic substrates, etc. In the method of moments (MoM), the volume–surface integral equation (VSIE) [1] is more advantageous than the surface integral equations (SIE) for mixed targets with arbitrarily inhomogeneous and anisotropic dielectric materials [2, 3]. However, the VSIE is discretized into a dense matrix equation through the MoM. An iterative solver needs $O(N^2)$ operations for the matrix-vector product (MVP) in each iteration, and requires $O(N^2)$ memory to store all the matrix elements, where N is the

number of unknowns. So the conventional MoM suffers from tremendously high computational cost and memory cost when the electrical size of the targets is large. Fortunately, many methods have been proposed in the past decades to deal with this problem, such as multilevel fast multipole algorithm (MLFMA) [4, 5], the adaptive integral method (AIM) [2, 6], and the pre-corrected fast Fourier transform (P-FFT) method [3, 7].

Recently, the equivalent dipole-moment method (EDM) [8–11] has been developed to simplify and accelerate the impedance matrix element filling procedure for the MoM. The EDM is based on the commonly used Rao–Wilton–Glisson (RWG) [12] and Schaubert–Wilton–Glisson (SWG) [13] basis functions, in which each RWG triangle pair or SWG tetrahedron pair is viewed as a dipole model with an equivalent dipole moment. The main advantage of EDM is that the impedance matrix element can be expressed in an extremely simplified form, which avoids the integral operators and saves the matrix-fill time, whereas the memory requirement and the matrix-solve time do not change.

Correspondence to: C. Gu; e-mail: gucq0138@sina.com
DOI 10.1002/mmce.20620
Published online 27 March 2012 in Wiley Online Library (wileyonlinelibrary.com).

More recently, fast dipole method (FDM) [14] based on the concept of the EDM is developed to mitigate this problem. In the FDM, the distance R between the interacting equivalent dipoles is expanded by a simple Taylor's series, and the interaction between the equivalent dipoles can be transformed into an aggregation–translation–disaggregation form naturally, which reduces the complexity of MVP between far-group pair, such as group i and group j , from $O(N_i N_j)$ to $O(N_i + N_j)$, where N_i and N_j are the numbers of the dipoles in groups i and j , respectively. In Ref. 15, the multilevel fast dipole method (MLFDM) is developed to solve the combined field integral equation (CFIE) for the perfect electric conducting (PEC) targets by using the multilevel grouping scheme [16]. The complexity of MVP and the memory requirement can be further reduced, as the multilevel grouping scheme is used in the MLFDM. Then, the FDM is improved through expanding the terms R^α ($\alpha = 1, -1, -2, -3$) and $\hat{\mathbf{R}}\hat{\mathbf{R}}$ in the formulation of the EDM using a simple Taylor's series [17]. The improved FDM (IFDM) can represent the interaction between two dipoles as an aggregation–translation–disaggregation form more accurately than the conventional FDM. In this article, the IFDM is extended to multilevel version and is applied to solve the VSIE efficiently for the electromagnetic (EM) scattering from 3D composite conducting-dielectric targets. Furthermore, a new empirical criterion for the far-group pairs at each level is given. The MLFMA has been successfully applied [4, 5, 16], which is based on the addition theorem and can achieve $O(N \log N)$ complexity and memory requirement, where N is the number of the unknowns. Compared with the MLFMA, the formula derivation and coding procedure of the MLFDM is much easier, although the MLFMA is more efficient than the MLFDM.

The remainder of the article is organized as follows. In Section II, the formulations of the VSIE for the composite targets including conductors and anisotropic dielectric materials is presented. Then the EDM for the VSIE is illustrated in Section III. In Section IV, the detail of the principle and implementation of the MLFDM to speed up the VSIE is represented. In Section V, some numerical results are given to verify the efficiency and accuracy of the algorithm. Finally, conclusions are drawn in Section VI.

II. FORMULATIONS OF THE VOLUME–SURFACE INTEGRAL EQUATION

Consider an arbitrarily shaped 3D scattering target, which consists of anisotropic dielectric material and conducting objects illuminated by an incident wave \mathbf{E}^i . Using the equivalence principle, the conducting targets and the dielectric materials can be replaced by equivalent surface current $\mathbf{J}_s(\mathbf{r})$ and equivalent volume current $\mathbf{J}_v(\mathbf{r})$, respectively. The scattered electric field $\mathbf{E}_s^s(r)$ and $\mathbf{E}_v^s(r)$ produced by the equivalent surface and volume current can be expressed as

$$\mathbf{E}_u^s(\mathbf{r}) = -j\omega\mathbf{A}_u(\mathbf{r}) - \nabla\phi_u(\mathbf{r}), \quad u = s, v \quad (1)$$

where

$$\mathbf{A}_u(\mathbf{r}) = \mu_0 \int_u \mathbf{J}_u(\mathbf{r}') G(\mathbf{r}, \mathbf{r}') du', \quad u = s, v \quad (2)$$

$$\phi_u(\mathbf{r}) = -\frac{1}{j\omega\epsilon_0} \int_u \nabla' \cdot \mathbf{J}_u(\mathbf{r}') G(\mathbf{r}, \mathbf{r}') du', \quad u = s, v \quad (3)$$

are the vector and scalar potentials produced by the equivalent currents, respectively. $G(\mathbf{r}, \mathbf{r}') = e^{-jk|\mathbf{r}-\mathbf{r}'|}/(4\pi|\mathbf{r}-\mathbf{r}'|)$ denotes the free-space Green's function, and ϵ_0 is the free-space permittivity.

The volume current $\mathbf{J}_v(\mathbf{r})$ is related to the total electric flux density $\mathbf{D}_v(\mathbf{r})$ via [5] the following equation

$$\mathbf{J}_v(\mathbf{r}) = j\omega\bar{\mathbf{k}}(\mathbf{r}) \cdot \mathbf{D}_v(\mathbf{r}), \quad (4)$$

where $\bar{\mathbf{k}}(\mathbf{r})$ is the contrast ratio expressed by

$$\bar{\mathbf{k}}(\mathbf{r}) = \mathbf{I} - \bar{\epsilon}_r^{-1}(\mathbf{r}) \quad (5)$$

with $\bar{\epsilon}_r(\mathbf{r})$ is the relative permittivity tensor of the electric anisotropic media, and \mathbf{I} is the unit tensor.

Then the VSIE can be constructed by the boundary conditions on the conductor surface \mathbf{S} and in the dielectric region \mathbf{V} [1–3].

$$(\mathbf{E}^i(\mathbf{r}) + \mathbf{E}_s^s(\mathbf{r}) + \mathbf{E}_v^s(\mathbf{r}))|_{\text{tan}} = 0, \quad \mathbf{r} \in \mathbf{S}, \quad (6)$$

$$\mathbf{E}(\mathbf{r}) = \mathbf{E}^i(\mathbf{r}) + \mathbf{E}_s^s(\mathbf{r}) + \mathbf{E}_v^s(\mathbf{r}), \quad \mathbf{r} \in \mathbf{V}, \quad (7)$$

where $\mathbf{E}(\mathbf{r}) = \bar{\epsilon}^{-1}(\mathbf{r}) \cdot \mathbf{D}_v(\mathbf{r})$ denotes the total electric field in the dielectric region \mathbf{V} , and $\bar{\epsilon}(\mathbf{r})$ is the permittivity tensors.

To apply the MoM to solve Eqs. (6) and (7), first the conductor surface \mathbf{S} and the dielectric region \mathbf{V} are discretized into small triangular patches and tetrahedral elements, respectively. Then the unknown surface and volume currents $\mathbf{J}_s(\mathbf{r})$ and $\mathbf{J}_v(\mathbf{r})$ can be expanded by a set of RWG and SWG basis functions, respectively, as

$$\mathbf{J}_s(\mathbf{r}) = \sum_{n=1}^{N_s} I_{sn} \mathbf{f}_{sn}(\mathbf{r}), \quad (8)$$

$$\mathbf{J}_v(\mathbf{r}) = \sum_{n=1}^{N_v} I_{vn} \bar{\mathbf{k}}_{vn} \cdot \mathbf{f}_{vn}(\mathbf{r}), \quad (9)$$

where $\mathbf{f}_{sn}(\mathbf{r})$ and $\mathbf{f}_{vn}(\mathbf{r})$ represent the n th RWG basis function and the n th SWG basis function, respectively. I_{sn} and I_{vn} are the unknown expansion coefficients. N_s and N_v are the numbers of RWG basis functions and SWG basis functions, respectively. $\bar{\mathbf{k}}_{vn}$ is the contrast ratio in the n th SWG basis function.

Substituting Eqs. (1)–(5) and Eqs. (8) and (9) into Eq. (6) and Eq. (7), then the Galerkin's method is employed to discretize Eq. (6) and Eq. (7). Finally, the matrix equations can be obtained

$$\sum_{n=1}^{N_s} I_{sn} \mathbf{Z}_{mn}^{ss} + \sum_{n=1}^{N_v} I_{vn} \mathbf{Z}_{mn}^{sv} = V_{sm}, \quad m = 1 \sim N_s, \quad (10a)$$

$$\sum_{n=1}^{N_s} I_{sn} Z_{mn}^{vs} + \sum_{n=1}^{N_v} I_{vn} Z_{mn}^{vv} = V_{vm}, \quad m = 1 \sim N_v, \quad (10b)$$

where

$$Z_{mn}^{ss} = -\langle \mathbf{f}_{sm}(\mathbf{r}), \mathbf{E}_{sn}^s(\mathbf{r}) \rangle \quad (11a)$$

$$Z_{mn}^{sv} = -\langle \mathbf{f}_{sm}(\mathbf{r}), \mathbf{E}_{vn}^v(\mathbf{r}) \rangle \quad (11b)$$

$$Z_{mn}^{vs} = -\langle \mathbf{f}_{vm}(\mathbf{r}), \mathbf{E}_{sn}^s(\mathbf{r}) \rangle \quad (11c)$$

$$Z_{mn}^{vv} = -\langle \mathbf{f}_{vm}(\mathbf{r}), \mathbf{E}_{vn}^v(\mathbf{r}) \rangle + \frac{1}{j\omega\epsilon_0} \langle \mathbf{f}_{vm}(\mathbf{r}), \bar{\epsilon}_r^{-1}(\mathbf{r}) \cdot \mathbf{f}_{vn}(\mathbf{r}) \rangle \quad (11d)$$

are the impedance matrix elements.

$$V_{sm} = \langle \mathbf{f}_{sm}(\mathbf{r}), \mathbf{E}^i(\mathbf{r}) \rangle \quad (12a)$$

$$V_{vm} = \langle \mathbf{f}_{vm}(\mathbf{r}), \mathbf{E}^i(\mathbf{r}) \rangle \quad (12b)$$

are the right-hand side vector elements for SIE and VIE respectively.

Equation (10) can be rewritten in a matrix form

$$\begin{bmatrix} \mathbf{Z}_{SS} & \mathbf{Z}_{SV} \\ \mathbf{Z}_{VS} & \mathbf{Z}_{VV} \end{bmatrix} \begin{bmatrix} \mathbf{I}_S \\ \mathbf{I}_V \end{bmatrix} = \begin{bmatrix} \mathbf{V}_S \\ \mathbf{V}_V \end{bmatrix}, \quad (13)$$

where \mathbf{Z}_{SS} , \mathbf{Z}_{SV} , \mathbf{Z}_{VS} , and \mathbf{Z}_{VV} are the impedance submatrices. \mathbf{I}_S , \mathbf{I}_V and \mathbf{V}_S , \mathbf{V}_V are the current and voltage vectors for SIE and VIE respectively.

III. THE EQUIVALENT DIPOLE-MOMENT METHOD FOR THE VSIE

The basic idea of the EDM [8–11] is that the fields radiated by the current on a RWG element or in a SWG element can be approximated as the fields due to an infinitely small dipole with an equivalent moment, beyond a threshold distance. The threshold distance is about $0.15\lambda_0$ (λ_0 is the wavelength in free-space) [9] for the triangle patches when the edge length of triangles is less than $0.1\lambda_0$. And threshold distance is approximately $0.15\lambda_g$ (λ_g is the wavelength in dielectric) [10, 11] for the tetrahedral cells when the edge length of tetrahedrons is less than $0.1\lambda_g$. Based on this assumption, the interaction of two basis functions can be replaced by the interaction of two infinitely small dipoles, except when they are very close to each other.

On the conducting surface S , the equivalent dipole moment [9, 12] on the n th RWG elements can be obtained by the integration of the surface current over the element surface T_{sn}^{\pm} .

$$\mathbf{m}_{sn} = \int_{T_{sn}^{\pm}} \mathbf{f}_{sn}(\mathbf{r}') ds' \approx l_{sn}(\mathbf{r}_{sn}^{c-} - \mathbf{r}_{sn}^{c+}), \quad (14)$$

where \mathbf{r}_{sn}^{\pm} are the position vectors of the centroid of T_{sn}^{\pm} defined in the global coordinate. It can be seen from Eq. (14) that the equivalent dipole moment of a RWG element can be simply represented by its geometric parameters.

In the dielectric region V , the equivalent dipole moment [11, 13] in the n th SWG elements can also be obtained by the integration of the volume current over the tetrahedron pair T_{vn}^{\pm} .

$$\mathbf{m}_{vn} = \int_{T_{vn}^{\pm}} \bar{\mathbf{k}}_{vn} \cdot \mathbf{f}_{vn}(\mathbf{r}') dv' \approx a_{vn} \bar{\mathbf{k}}_{vn}^+ \cdot (\mathbf{r}_{vns}^c - \mathbf{r}_{vn}^{c+}) + a_{vn} \bar{\mathbf{k}}_{vn}^- \cdot (\mathbf{r}_{vn}^{c-} - \mathbf{r}_{vns}^c), \quad (15)$$

where \mathbf{r}_{sn}^{\pm} are the position vectors of the centroid of T_{vn}^{\pm} and \mathbf{r}_{vns}^{\pm} is the position vectors of the centroid of the common face S_{vn} of the T_{vn}^{\pm} . It can be seen from Eq. (15) that the equivalent dipole moment of the volume current in the n th SWG element not only includes its geometric parameters but also contains the dielectric information.

Referring to Refs. [10, 11], the radiated electric fields of the n th infinitesimal dipole associated to the n th RWG element or the n th SWG element at the field point \mathbf{r} can be expressed as

$$\mathbf{E}_{un}^s = \frac{\eta e^{-jkR}}{4\pi} \left[\hat{\mathbf{R}}(\hat{\mathbf{R}} \cdot \mathbf{m}_{un}) \left(\frac{jk}{R} + 3C \right) - \mathbf{m}_{un} \left(\frac{jk}{R} + C \right) \right], \quad u = s, v \quad (16)$$

where $\mathbf{R} = \mathbf{r} - \mathbf{r}_{un}$ is the vector from the center point \mathbf{r}_{un} of the n th equivalent dipole to the field point \mathbf{r} . $R = |\mathbf{R}|$, $\hat{\mathbf{R}} = \mathbf{R}/R$. $\mathbf{r}_{un} = (\mathbf{r}_{un}^{c+} + \mathbf{r}_{un}^{c-})/2$ and $C = [1 + 1/(jkR)]/R^2$.

Substituting Eq. (16) into Eq. (11), and furthermore Eq. (13) is rewritten as

$$[\mathbf{Z}][\mathbf{I}] = [\mathbf{V}], \quad (17)$$

where \mathbf{Z} is constituted by the submatrices \mathbf{Z}_{SS} , \mathbf{Z}_{SV} , \mathbf{Z}_{VS} , and \mathbf{Z}_{VV} . $\mathbf{I} = [\mathbf{I}_S, \mathbf{I}_V]^T$, $\mathbf{V} = [\mathbf{V}_S, \mathbf{V}_V]^T$. And the impedance elements Z_{mn} of the impedance matrix \mathbf{Z} can be expressed in a simple form that

$$Z_{mn} = \frac{\eta e^{-jkR}}{4\pi} \left[\mathbf{m}'_m \cdot \mathbf{m}_n \left(\frac{jk}{R} + C \right) - (\mathbf{m}'_m \cdot \hat{\mathbf{R}})(\hat{\mathbf{R}} \cdot \mathbf{m}_n) \left(\frac{jk}{R} + 3C \right) \right], \quad (18)$$

in which $\mathbf{R} = \mathbf{r}_{mn} = \mathbf{r}_m - \mathbf{r}_n$ is the vector from the center point \mathbf{r}_n of the n th equivalent dipole to the center point \mathbf{r}_m of the m th equivalent dipole.

$$\mathbf{m}_n = \begin{cases} l_n(\mathbf{r}_n^{c-} - \mathbf{r}_n^{c+}) & T_n^{\pm} \in S \\ a_n \bar{\mathbf{k}}_n^+ \cdot (\mathbf{r}_{ns}^c - \mathbf{r}_n^{c+}) + a_n \bar{\mathbf{k}}_n^- \cdot (\mathbf{r}_n^{c-} - \mathbf{r}_{ns}^c) & T_n^{\pm} \in V \end{cases} \quad (19)$$

is the n th equivalent dipole moment for the current in the RWG or SWG elements. And

$$\mathbf{m}'_n = \begin{cases} l_n(\mathbf{r}_n^{c-} - \mathbf{r}_n^{c+}) & T_n^{\pm} \in S \\ a_n(\mathbf{r}_n^{c-} - \mathbf{r}_n^{c+}) & T_n^{\pm} \in V \end{cases} \quad (20)$$

is the n th moment of the RWG or SWG basis function. It can be seen that $\mathbf{m}'_n = \mathbf{m}_n$ for the RWG basis functions, while $\mathbf{m}'_n \neq \mathbf{m}_n$ for the SWG basis functions.

As can be seen from the above equations, when any two basis functions are with a threshold distance, the impedance matrix elements between them do not contain integral operators using the EDM. Thus the EDM can greatly simplify the matrix filling process and save computation time. In this article, the threshold distance is chosen as $0.2\lambda_0$.

IV. ACCELERATED SOLUTION USING MULTILEVEL FAST DIPOLE METHOD

To implement the MLFDM, the entire target needs multilevel grouping [16] first. The whole target can be wrapped by a cube with the size of $2^L\Delta$, in which Δ is the size of cube at the finest level and L is the minimal number to meet the condition of wrapping the target by $2^L\Delta$ sized cube. Then the $2^L\Delta$ sized cube is partitioned into eight equal sub-cubes, which forms the first level (Level 1) group, and each sub-cube is then recursively subdivided into eight smaller cubes until the edge length of the finest cube is Δ exactly. In this way, the L -level grouping procedure from Level 1 to Level L is obtained. The size of the cube at Level l is $\Delta_l = 2^{L-l}\Delta$.

Depending on the distance between two groups at the same level, we define two regions for each group. N_i and F_i denote the near and far regions of group i separately. If group j is in the N_i , group j and group i are called near-group pair, otherwise are called far-group pair. In our method, the number of interval groups $D(i,j) = \max\{|x_i - x_j|, |y_i - y_j|, |z_i - z_j|\}/d$ between group i and group j at the same level is used to decide whether the two groups are near-group pair or far-group pair, where (x_i, y_i, z_i) and (x_j, y_j, z_j) are the coordinates of the centroid of group i and group j , respectively, and d is the side length of the group at this level. For example, if $D(i,j) \leq D_b$, group i and group j are the near-group pair, else the two groups are far-group pair, where D_b is a given number. The value of D_b affects the efficiency and accuracy of the MLFDM. According to our experiments, we give an empirical criterion for different levels

$$D_b(l) = \lceil 1.5\Delta_l/\lambda_0 \rceil + 2. \quad (21)$$

where $\lceil \lambda \rceil$ is the ceil function, Δ_l is the size of the group at Level l . The empirical criterion is different from the one in Ref. [15], because the IFDM is employed and the targets not only includes the PEC objects but also includes the dielectric objects. And we remark that the new empirical criterion for the multilevel IFDM also can be used to solve the CFIE for the PEC targets. We mention that in practical applications the values of $D_b(l)$ at each level can be adjusted to satisfy the required accuracy.

Now, we consider two equivalent dipoles m ($m \in j$) and n ($n \in i$) and suppose group i and group j are far-group pair ($i \in F_j$ or $j \in F_i$). The distance $R = |\mathbf{r}_{mn}| = |\mathbf{r}_m - \mathbf{r}_n|$ between the centers of the two equivalent dipoles definitely satisfies the approximation rule of the EDM and

the impedance element Z_{mn} can be represented by Eq. (18) and it can be rewritten as

$$Z_{mn} = \mathbf{m}'_m \cdot \mathbf{T}(\mathbf{r}_m, \mathbf{r}_n) \cdot \mathbf{m}_n, \quad (22)$$

where

$$\mathbf{T}(\mathbf{r}_m, \mathbf{r}_n) = \frac{\eta e^{-jkR}}{4\pi} \left[\mathbf{I} \left(jkR^{-1} + R^{-2} + \frac{1}{jk}R^{-3} \right) - \hat{\mathbf{R}}\hat{\mathbf{R}} \left(jkR^{-1} + 3R^{-2} + \frac{3}{jk}R^{-3} \right) \right]. \quad (23)$$

The key idea of the FDM [14] and the improved fast dipole method (IFDM) [17] is expanding the term $\mathbf{T}(\mathbf{r}_m, \mathbf{r}_n)$ through Taylor series to achieve the separation of the field dipole and source dipole. Now we introduce the IFDM in detail.

The vector \mathbf{r}_{mn} can be rewritten as $\mathbf{R} = \mathbf{r}_{mn} = \mathbf{r}_{ji} + \mathbf{r}_{mj} - \mathbf{r}_{ni}$, in which $\mathbf{r}_{ji} = \mathbf{r}_{o_j} - \mathbf{r}_{o_i}$, $\mathbf{r}_{mj} = \mathbf{r}_m - \mathbf{r}_{o_j}$, $\mathbf{r}_{ni} = \mathbf{r}_n - \mathbf{r}_{o_i}$, \mathbf{r}_{o_i} and \mathbf{r}_{o_j} are the center positions of group i and group j , and \mathbf{r}_m and \mathbf{r}_n are the center positions of the m th and n th equivalent dipoles.

So R^α ($\alpha = 1, -1, -2, -3$) in Eq. (23) can be expanded using the Taylor series as [17]

$$\begin{aligned} R^\alpha &= |\mathbf{R}|^\alpha = |\mathbf{r}_{ji} + \mathbf{r}_{mj} - \mathbf{r}_{ni}|^\alpha \\ &\approx r_{ji}^\alpha \left[1 + \alpha \left(\frac{\hat{\mathbf{r}}_{ji} \cdot \mathbf{r}_{mj}}{r_{ji}} + \frac{r_{mj}^2 + (\alpha - 2)(\mathbf{r}_{ji} \cdot \mathbf{r}_{mj})^2}{2r_{ji}^2} \right) \right. \\ &\quad \left. + \alpha \left(\frac{\hat{\mathbf{r}}_{ij} \cdot \mathbf{r}_{ni}}{r_{ij}} + \frac{r_{ni}^2 + (\alpha - 2)(\mathbf{r}_{ij} \cdot \mathbf{r}_{ni})^2}{2r_{ij}^2} \right) \right] \end{aligned} \quad (24)$$

And the dyad term $\hat{\mathbf{R}}\hat{\mathbf{R}}$ in Eq. (23) can be approximately expressed as [17]

$$\hat{\mathbf{R}}\hat{\mathbf{R}} = \frac{\mathbf{R}\mathbf{R}}{R^2} \approx \frac{1}{r_{ji}^2} [\mathbf{r}_{ji}\mathbf{r}_{ji} + \mathbf{s}\mathbf{s}], \quad (25)$$

where

$$\mathbf{s} = (\mathbf{r}_{mj} - \mathbf{r}_{ni}) - (\mathbf{r}_{mj} - \mathbf{r}_{ni}) \cdot \hat{\mathbf{r}}_{ji}\hat{\mathbf{r}}_{ji}. \quad (26)$$

Substituting Eqs. (24)–(26) into Eq. (22), the separation of the field dipole and source dipole can achieve, and the impedance matrix element for the VSIE is transformed into an aggregation–translation–disaggregation form. The transfer function only depends on the vector \mathbf{r}_{ji} . In other words, all the aggregation and disaggregation functions in group i and j share the same transfer function. So the calculation process of the MVP for far-group interactions can be naturally divided into three steps: aggregation, transfer, and disaggregation, which speed up the MVP remarkably (see Fig. 1). Assuming that there are N_i (N_j) unknowns in group i (group j), the computational complexity of the interactions between group i and group j can be reduced from $O(N_i N_j)$ to $O(N_i + N_j)$.

Now we introduce the MLFDM in detail and assume that the target is divided into L levels (from Level 1 to

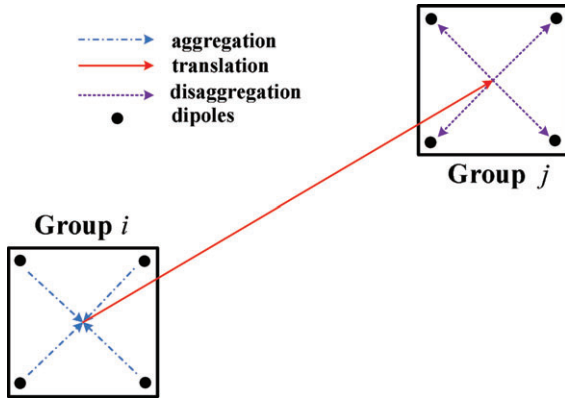


Figure 1 The aggregation, transfer, and disaggregation between the far-group pair group i and group j . [Color figure can be viewed in the online issue, which is available at wileyonlinelibrary.com.]

Level L). An equivalent dipole element m resides in group j_l at Level l , in which group j_l represents the j_l th group containing element m at Level l ($0 \leq j_l \leq 8^l - 1$). Under these assumptions, it is easy to know that group j_{l-1} at Level $(l - 1)$ is the father group of group j_l at Level l . Then the MVP can be divided into two steps by the L -level MLFDM as

- Step 1: From Level 2 to Level L , all those far-group pairs (i_l, j_l) , $(i_l \in R_l)$, need to be handled using eqs. (22)–(25). The aggregation, translation, and disaggregation processes occur in every such group pair. Here, $R_l = \{i_l | i_l \in F_{j_l}, i_{l-1} \in N_{j_{l-1}}\}$ is a set of groups at Level l , in which i_l must meet the conditions that groups i_l and j_l are the far-group pair, and their farther groups i_{l-1} and j_{l-1} are the near-group pair.

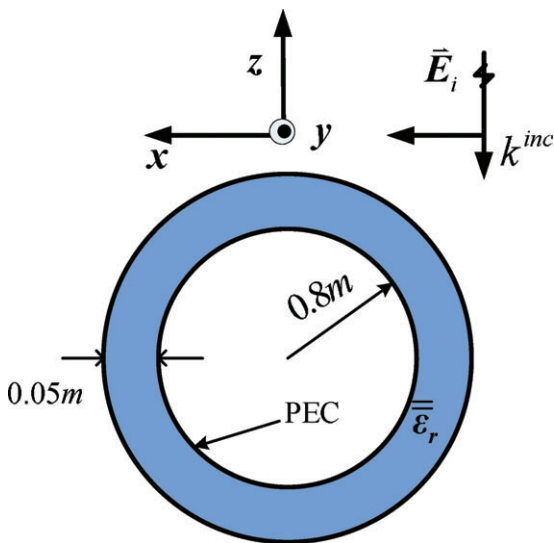


Figure 2 Geometry of a PEC sphere covered by spherical dielectric shell for the first problem. [Color figure can be viewed in the online issue, which is available at wileyonlinelibrary.com.]

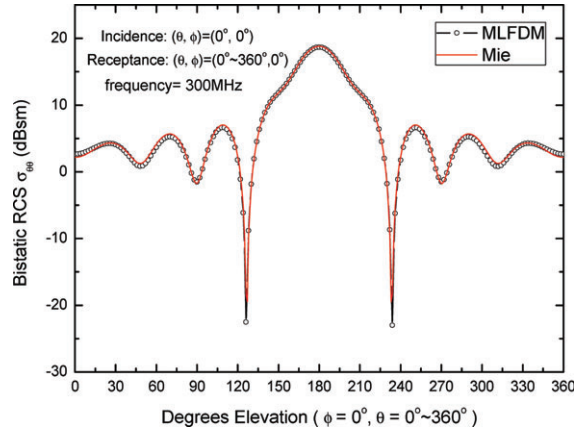


Figure 3 Bistatic RCSs in $\theta\theta$ polarization of a PEC sphere covered by spherical dielectric shell illuminated by a uniform plane wave with the incident direction of $(\theta, \phi) = (0^\circ, 0^\circ)$. [Color figure can be viewed in the online issue, which is available at wileyonlinelibrary.com.]

- Step 2: At the finest level (Level L), all the near region interactions are calculated directly. In other words, all near-group pairs at the finest level (i_L, j_L) , $(i_L \in N_{j_L})$, need to be handled. The conventional MoM [Eq. (11)] or the EDM [Eq. (18)] are used depending on the distance between each two dipoles.

Considering the aggregation, translation, and disaggregation functions are very simple, so these functions are not stored in the MLFDM, which are calculated in the iterative computation if needed. And only the near interactions at the finest level are stored. So the MLFDM is lower consumed for memory than the EDM and the conventional MoM.

V. NUMERICAL RESULTS

In this section, some numerical results are presented to validate the accuracy and efficiency of the MLFDM. We remark that in the following examples, the generalized minimum residual (GMRES) iterative solver and the block diagonal preconditioner (BDP) are used to obtain an identical residual error ≤ 0.005 . And all the simulations are performed on a personal computer with the Intel(R)

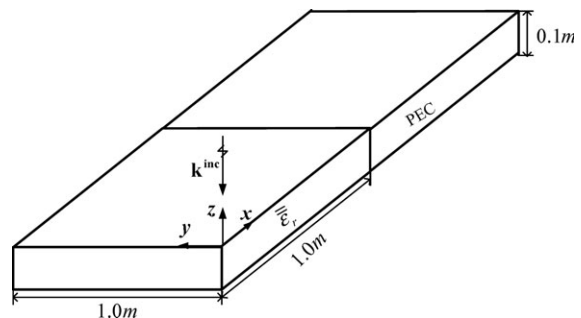


Figure 4 Geometry of a composite conducting-dielectric target for the second problem.

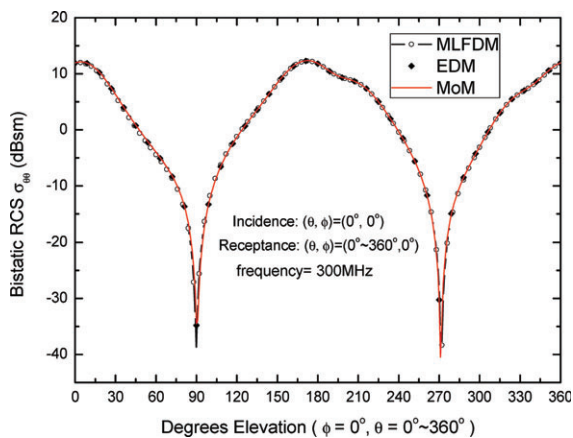


Figure 5 Bistatic RCSs in $\theta\theta$ polarization of a composite conducting-dielectric target illuminated by a uniform plane wave with the incident direction of $(\theta, \phi) = (0^\circ, 0^\circ)$. [Color figure can be viewed in the online issue, which is available at wileyonlinelibrary.com.]

Pentium(R) Dual-Core CPU E5500 with 2.80 GHz (only one core is used) and 2.0 GB RAM.

For the first problem, the bistatic RCSs of a PEC sphere covered by spherical dielectric shell ($\bar{\epsilon}_r = 1.5\mathbf{I}$) are

TABLE I Total CPU Time and Memory Requirement of the Conventional MoM, the EDM, and the MLFDM

Method		MoM	EDM	MLFDM
Problem 1	Memory (MB)	–	–	524
	CPU time (s)	–	–	1046
Problem 2	Memory (MB)	401	401	102
	CPU time (s)	472	129	89

calculated. The radius of the PEC sphere is 0.8 m and the thickness of the shell is 0.05 m shown in Figure 2. The total number of unknowns is 22,297 including 3534 RWG and 18,763 SWG basis functions. The size of the finest group is 0.12 m and a 4-level MLFDM is used. The bistatic RCS for the $\theta\theta$ polarization is calculated and compared with the Mie solutions. These two results are in good agreement shown in Figure 3. The number of iterations required by the GMRES is 94. And the EDM and the conventional MoM cannot be used to calculate the problem in this computer for 2.0 GB RAM is not enough for the EDM and the MoM.

In the second problem, the bistatic RCSs of a composite conducting-dielectric target (see Fig. 4) are considered. The target is constituted by one PEC slab and one dielectric slab with the same size $1.0\text{ m} \times 1.0\text{ m} \times 0.1\text{ m}$. The

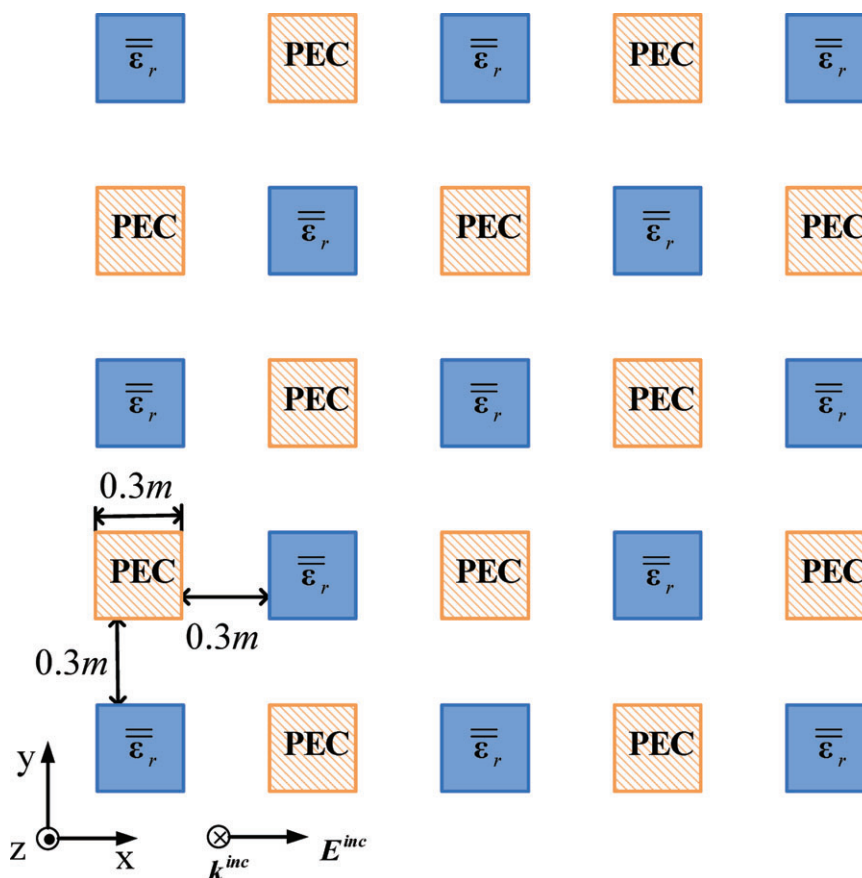


Figure 6 Geometry of a 5×5 array including conducting array elements and dielectric array elements for the last problem. [Color figure can be viewed in the online issue, which is available at wileyonlinelibrary.com.]

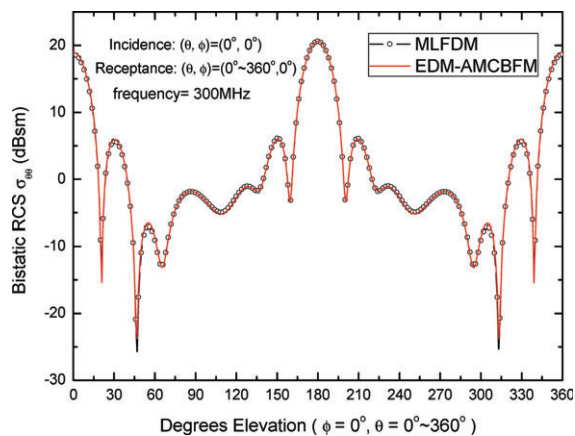


Figure 7 Bistatic RCSs in $\theta\theta$ polarization of a 5×5 array including conducting array elements and dielectric array elements illuminated by a uniform plane wave with the incident direction of $(\theta, \phi) = (0^\circ, 0^\circ)$. [Color figure can be viewed in the online issue, which is available at wileyonlinelibrary.com.]

relative permittivity of the dielectric slab is $\bar{\epsilon}_r = [1.5, 0, 0; 0, 1.5, 0; 0, 0, 2.0]$. The total number of unknowns is 7106 including 1701 RWG basis functions and 5405 SWG basis functions. A 5-level MLFDM is used and the group at the finest level is with the size of 0.1 m. The bistatic RCS in $\theta\theta$ polarization calculated by the MLFDM is compared with the EDM and the conventional MoM shown in Figure 5.

Table I summarizes the total CPU time and memory requirement of the conventional MoM, the EDM, and the MLFDM for the above two simulation examples. It can be seen that the MLFDM saves much memory and CPU time compared with the EDM and the conventional MoM.

Finally, the bistatic RCSs of a 5×5 array including conducting array elements and dielectric array elements, shown in Figure 6, are considered. All the array elements have the same size $0.3 \text{ m} \times 0.3 \text{ m} \times 0.3 \text{ m}$, and the gap between two adjacent elements is 0.3 m. All the dielectric elements have the same relative permittivity which is $\bar{\epsilon}_r = [2.0, 0, 0; 0, 2.0, 0; 0, 0, 1.5]$. The total number of unknowns is 17,157 including 3456 RWG basis functions and 13,701 SWG basis functions. A 5-level MLFDM is used and the group at the finest level is with the size of 0.1 m. the bistatic RCSs are investigated using the MLFDM and the EDM-AMCBFM [18]. And excellent agreements are observed in Figure 7. It costs 301 s and 182 MB memory using the MLFDM, whereas needs 1691 s and 191 MB memory using the hybrid EDM-AMCBFM. Here, a stricter current criterion is used for the EDM-AMCBFM, which is $\epsilon = \frac{\|\mathbf{I}^{T(k+1)} - \mathbf{I}^{T(k)}\|_2}{\|\mathbf{I}^{T(k)}\|_2} \times 100\%$, where $\|\bullet\|_2$ is the vector-2 norm. In this article, the current criterion ϵ of the EDM-AMCBFM is chosen as 2%, and the 6th-level total current is calculated.

VI. CONCLUSIONS

In this article, the IFDM is extended to the multilevel version and applied to accelerate solving electromagnetic scattering by the composite targets including conductors

and dielectric objects using the VSIE. And a new empirical criterion for far-group pairs at each level is given, which can be used in PEC objects, dielectric objects, and the composite objects when the multilevel IFDM is employed. The computational complexity and memory requirement can be reduced remarkably by the MLFDM. Furthermore, the MLFDM is based on the concept of the EDM and it is very simple for implementation. Numerical results show that the MLFDM can obtain satisfactory results for practical engineering applications.

ACKNOWLEDGMENT

The work is supported by the National Nature Science Foundation of China under Grant No. 61071019 and the Funding of Jiangsu Innovation Program for Graduate Education under Grant No. CXZZ11_0229.

REFERENCES

1. C.C. Lu and W.C. Chew, A coupled surface-volume integral equation approach for the calculation of electromagnetic scattering from composite metallic and material targets, *IEEE Trans Antennas Propag* 48 (2000), 1866–1868.
2. W.B. Ewe, L.W. Li, and M.S. Leong, Fast solution of mixed dielectric/conducting scattering problem using volume-surface adaptive integral method, *IEEE Trans Antennas Propag* 52 (2004), 3071–3077.
3. X.C. Nie, N. Yuan, L.W. Li, Y.B. Gan, and T.S. Yeo, A fast volume-surface integral equation solver for scattering from composite conducting-dielectric objects, *IEEE Trans Antennas Propag* 53 (2005), 818–824.
4. J.M. Song, C.C. Lu, and W.C. Chew, Multilevel fast multipole algorithm for electromagnetic scattering by large complex objects, *IEEE Trans Antennas Propag* 45 (1997), 1488–1493.
5. G. Kobidze and B. Shanker, Integral equation based analysis of scattering from 3-D inhomogeneous anisotropic bodies, *IEEE Trans Antennas Propag* 52 (2004), 2650–2658.
6. C.F. Wang, F. Ling, J. Song, and J.-M. Jin, Adaptive integral solution of combined field integral equation, *Microwave Opt Technol Lett* 19 (1998), 321–328.
7. J.R. Phillips and J.K. White, A precorrected-FFT method for electrostatic analysis of complicated 3-D structures, *IEEE Trans Comput Aided Design Integr Circuits Syst* 16 (1997), 1059–1072.
8. S.N. Makarov, *Antenna and EM modeling with MATLAB*, Wiley, New York, 2002.
9. J. Yeo, S. Köksoy, V.V.S. Prakash, and R. Mittra, Efficient generation of method of moments matrices using the characteristic function method, *IEEE Trans Antennas Propag* 52 (2004), 3405–3410.
10. J.D. Yuan, C.Q. Gu, and G.D. Han, Efficient generation of method of moments matrices using equivalent dipole-moment method, *IEEE Antennas Wireless Propag Lett* 8 (2009), 716–719.
11. J.D. Yuan, C.Q. Gu, and Z. Li, Electromagnetic scattering by arbitrarily shaped stratified anisotropic media using the equivalent dipole moment method, *Int J RF Microwave Comput Aided Eng* 20 (2010), 416–421.
12. S.M. Rao, D.R. Wilton, and A.W. Glisson, Electromagnetic scattering by surfaces of arbitrary shape, *IEEE Trans Antennas Propag* AP-30 (1982), 409–418.

13. D.H. Schaubert, D.R. Wilton, and A.W. Glisson, A tetrahedral modeling method for electromagnetic scattering by arbitrarily shaped inhomogeneous dielectric bodies, *IEEE Trans Antennas Propag AP-32* (1984), 77–85.
14. X.L. Chen, C.Q. Gu, Z.Y. Niu, and Z. Li, Fast dipole method for electromagnetic scattering from perfect electric conducting targets, to be published in *IEEE Trans Antennas Propag.*
15. X.L. Chen, Z. Li, Z.Y. Niu, and C.Q. Gu, Multilevel fast dipole method for electromagnetic scattering from perfect electric conducting targets, to be published in *IET Microwave Antennas Propag.*
16. W.C. Chew, J.M. Jin, E. Michielssen, and J.M. Song, *Fast and efficient algorithms in computational electromagnetics*, Artech House, Boston, MA, 2001.
17. X.L. Chen, Z. Li, Z.Y. Niu, and C.Q. Gu, Analysis of electromagnetic scattering from PEC targets using improved fast dipole method, *J Electromagn Waves Appl* 25 (2011), 2254–2263.
18. J.D. Yuan, C.Q. Gu, and G.D. Han, A hybrid equivalent dipole moment and adaptive modified characteristic basis function method for electromagnetic scattering by multilayered dielectric bodies, *Int J RF Microwave Comput Aided Eng* 19 (2009), 685–691.

BIOGRAPHIES



Xinlei Chen was born in Jiangsu, China, in 1984. He received B.E. and the M.E. degrees from Nanjing University of Aeronautics and Astronautics (NUAA), Nanjing, in 2007 and in 2010. Since April 2010 he has been with the College of Electronic and Information Engineering, Nanjing University of Aeronautics and Astronautics, China, where he is currently working toward the Ph.D. degree. His current research interest is fast integral equation methods.



Changqing Gu was born in Jiangsu, China, in 1958. He is a professor of electronic engineering at the Nanjing University of Aeronautics and Astronautics, China, and is the member of editorial board of Chinese journal of radio science. His current research interest is in the areas of broadband antenna, smart antenna, and computational electromagnetics.



Zhenyi Niu was born in Henan, China, in 1975. He received the B.E. and M.E. degrees from Nanjing University of Aeronautics and Astronautics (NUAA), Nanjing, China, in 1997 and 2000, respectively. He received the Ph.D. degree from the State Key Laboratory of Millimeter Waves, Department of Radio Engineering, Southeast University, Nanjing, China, in 2006. He is currently an Associate Professor in the College of Electronic and Information Engineering, NUAA. His research interests include electromagnetic compatibility, wave propagation, scattering, microwave circuit, and antenna design.



Zhuo Li was born in Hubei, China, in June 1979. He received B.E. and the M.E. degrees from Nanjing University of Aeronautics and Astronautics (NUAA), Nanjing, in 2001 and in 2004. He earned a Ph.D. at the State Key Laboratory of Millimeter Waves, Department of Radio Engineering, Southeast University, Nanjing, in 2009. He is currently working as a lecturer at NUAA. His research interests include computational electromagnetics, fast algorithms, electromagnetic compatibility and prediction of urban electromagnetic environment.